# Crystal structure of a protein phosphatase 2A heterotrimeric holoenzyme

Uhn Soo Cho[1] & Wenqing Xu[1]

[1]*Department of Biological Structure, University of Washington, Seattle, WA 98195*

## Supplementary Information

### Supplementary Methods

**Overexpression and purification of the catalytic C subunit**

Structural studies of PP2A were previously impossible because of the very low level of PP2A C subunit monomer (PP2Ac) that can be recovered, even from baculovirus insect cell or mammalian expression systems. The overall protein level of PP2Ac is decent in the cell. However, it is mostly in tight complexes with many other binding proteins. Isolating PP2Ac from those heterogeneous complexes was not straightforward and the isolated PP2Ac protein was unstable in solution. We have successfully isolated large amounts of stable PP2Ac for structural studies through two modifications. The first was introducing an uncleavable HA tag (8 residues) onto the N-terminus of the C subunit. For unclear reasons, the stability of the isolated PP2Ac was significantly improved[41]. The second was introducing a mutation in the active-site residues D88N or H118N[42], which significantly improved the expression level of PP2Ac to about 1 mg from 1 liter cells. It has been recently reported that PP2Ac can also be expressed with decent yields in baculovirus systems by adding an uncleavable $His_8$-tag to the N-terminus[43].

To produce the baculovirus for expression of the human catalytic Cα subunit, PP2A Cα was cloned into the pFastBac HTb vector with an N-terminal HA-tag and a TEV cleavage site. The point mutation of D88N was introduced to make an inactive PP2A Cα, and bacmids of this mutant were prepared from the Bac-to-Bac Baculovirus expression system (GibroBRL). Hi-5 cells in SF-900 II serum-free medium at a density of $2x10^6$ cells/$cm^2$ were infected with fresh recombinant virus and incubated at 27 °C for 72 h. The cells were collected by centrifugation at 1000 g for 20 min and pellets were washed with 50 mM Tris-HCl (pH8.0), 100 mM NaCl, 5 mM β-mercaptoethanol with protease inhibitors (PMSF, leu-peptin, Benzamidine) and stored at -80 °C. Freeze/thaw and mild sonication was used to lysate cells, and cell debris was removed by centrifugation at 26,000 g for 1 h. The soluble fraction was filtered with 0.8 μm syringe filters and applied to the Ni-NTA affinity column pre-equilibrated with 50 mM Tris-HCl (pH8.0), 100 mM NaCl, 3 mM β-mercaptoethanol. PP2A C subunit protein was eluted with elution buffer (50 mM Tris-HCl [pH8.0], 100 mM NaCl, 300 mM imidazole, 3 mM β-mercaptoethanol) and dialyzed overnight at 4 °C in 50 mM Tris-HCl (pH8.0), 100 mM

NaCl, 1 mM DTT. Dialyzed protein sample was incubated with TEV (1:20 w/w ratio) at room temperature overnight, and re-applied to Ni-NTA to remove cleaved His-tag fragments. Flow-through fraction of second Ni-NTA was dialyzed again with 50 mM Tris-HCl (pH8.0), 25 mM NaCl, 1 mM DTT and applied into a Hi-trap HQ 5 ml column (Amersham Biotech) pre-equilibrated with 50 mM Tris-HCl (pH8.0), 1 mM DTT. Bound protein was eluted by one-step elution with 50 mM Tris-HCl (pH8.0), 500 mM NaCl, 1 mM DTT. The elution fraction was applied to a Superdex 200 size-exclusion column (Amersham Biotech) pre-equilibrated with 25 mM Tris-HCl (pH8.0), 50 mM NaCl, 1 mM DTT. The purified C subunit was used for PP2A holoenzyme purification and other experiments.

**Overexpression and purification of A subunit and B56γ1 subunit**

Full-length mouse PP2A Aα subunit was cloned into pGEX4T1 vector (Amersham Biotech) with an N-terminal TEV cleavage site and expressed in *E. coli* strain BL21(DE3). Expression was induced by the addition of 0.1 mM IPTG at $O.D._{600}$=0.6 after dropping the temperature from 37 °C to 18 °C, and cells were grown for an additional 18 hours. Cells were then collected by centrifugation, lysated by sonication, and cell debris removed by centrifugation at 26,000 g for 1 h. The soluble fraction was filtered with 0.8 μm syringe filters and applied into a glutathione S transferase (GST) affinity column pre-equilibrated with 50 mM Tris-HCl (pH8.0), 100 mM NaCl, 3 mM β-mercaptoethanol. Proteins were eluted by one step elution with elution buffer (50 mM Tris-HCl [pH 8.0], 100 mM NaCl, 20 mM reduced-glutathione, 3 mM β-mercaptoethanol) and dialyzed overnight at 4 °C in 50 mM Tris-HCl (pH8.0), 100 mM NaCl, 1 mM DTT. The dialyzed protein sample was incubated with TEV (1:20 molar ratio) at room temperature overnight and re-applied to the GST affinity column to remove any cleaved GST-tag. Flow-through fraction of the second GST column was dialyzed again with 50 mM Tris-HCl (pH8.0), 50 mM NaCl, 1 mM DTT and applied into a Hitrap HQ 5 ml column (Amersham Biotech) pre-equilibrated with 50 mM Tris-HCl (pH8.0), 1 mM DTT. Bound protein was eluted by gradient elution up to 500mM NaCl. Elution fractions were concentrated and applied to a Superdex 200 size-exclusion column (Amersham Biotech) pre-equilibrated with 25 mM Tris-HCl (pH8.0), 50 mM NaCl, 1 mM DTT. The seleno-methionine (Se-Met)-labeled mouse PP2A Aα subunit was overexpressed in *E. coli* strain BL21 (DE3) by adapting a protocol originally designed for leaky expression of proteins. The overall purification procedure of Se-Met labeled A subunit was the same with native protein.

Human B56γ1 construct (30-437 a.a) was cloned into pGEX4T1 with a TEV cleavage site and expressed in *E. coli* strain BL21 (DE3). Overall purification procedure was the same at the A subunit. Se-Met labeled B56 subunit was prepared the same way at the Se-Met A subunit.

**Reconstitution and crystallization of the AαB56γ1Cα heterotrimeric complex**

PP2A holoenzyme heterotrimers were reconstituted by mixing highly purified A, B, and C subunits. All A subunits and most B subunits used for crystallization were overexpressed in *E. coli*, while all C subunits used were overexpressed in Hi-5 cells using baculovirus systems. To obtain diffractable heterotrimeric PP2A crystals, more than 50 A-B-C combinations were reconstituted, further purified and used for extensive screening

of crystallization conditions. Reconstituted heterotrimeric PP2A holoenzyme was purified by mixing each subunit with a 1:1:1 molar ratio and using the Superdex 200 size-exclusion column equilibrated with 30mM Tris-HCl (pH8.0), 50mM NaCl, 1mM DTT. As shown in Supplementary Fig. S1a, a single peak was observed in the size-exclusion chromatograph and stable heterotrimeric PP2A holoenzyme formation was confirmed by SDS-PAGE and Coomassie Brilliant Blue staining. The human Aα-B56γ1-Cα heterotrimeric complex was concentrated to ~ 8mg/ml with a threefold molar excess of microcystin-LR (MCLR), a specific PP2A inhibitor. The PP2A Aα/B56γ1/Cα-microcystin complex was crystallized in 0.1M MES (pH7.0), 50mM NaCl, 1.4M ammonium sulfate, 0.2M LiCl, 2% 1,6-diaminohexane. This crystal form initially diffracted to ~8 Å resolution with synchrotron radiation. Repeated seeding, crystal stabilization with additives and controlled dehydration gradually improved the diffraction limit of this crystal form to 3.5 Å resolution.

**Structural determination and analysis**

Partly because of the large size of this complex and the conformational change in the A subunit, we were not able to solve the structure by molecular replacement. Fast crystal decay during data collection prevented us from successfully performing a MAD experiment. The structure was solved by single anomalous dispersion method (SAD) using Se-Met substituted A subunit or both A and B subunits. In the final structure model, all residues except the following residues are included in the final structural model of one of the two complexes: residues 1-6 in the A subunit, residues 407-437 in the B subunit, the HA tag and residues 1-3 in the C subunit. The other complex in the asymmetric unit has more missing residues, including the C-terminal tail of the C-subunit, most likely because of crystal packing effect. These two AB'C complexes in the asymmmetric unit with an essentially identical architecture, with a rms difference of 1.5 Å, 1.1 Å and 0.5 Å in A, B and C subunits, respectively.

The A-C interface buries a structural interface of ~1,850 $Å^2$, while the A-B and B-C interfaces bury ~1,300 $Å^2$ and ~1,600 $Å^2$ of structural interfaces, respectively. The B-C interface includes the contribution of ~400 $Å^2$ from the C-terminal tail.

## Supplementary Figures and Legends

## Supplementary Figure S1

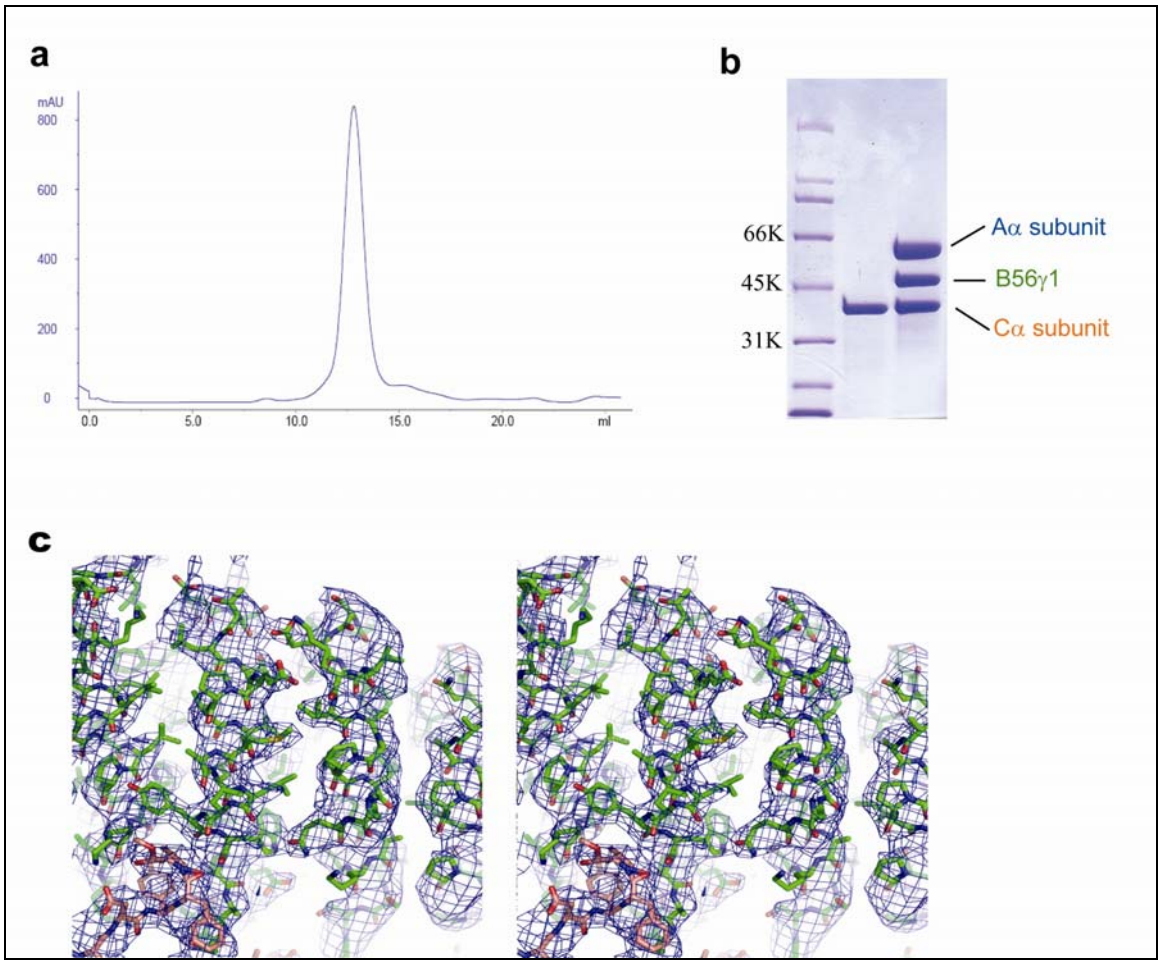


**Supplementary Figure S1. Purification and reconstitution of an AB'C heterotrimeric holoenzyme. a,** Reconstituted ABC holoenzyme demonstrated a single peak in SEC chromatograph. **b,** This peak shows a stoichiometric Aα-B56γ1-Cα complex in a SDS PAGE gel stained with Commassie Brilliant Blue. **c**, A stereo-view of the initial SAD experimental electron density map with 1σ level. B56γ1 is shown in green and the C-terminal tail of the catalytic Cα subunit is shown in orange.

## Supplementary Figure S2

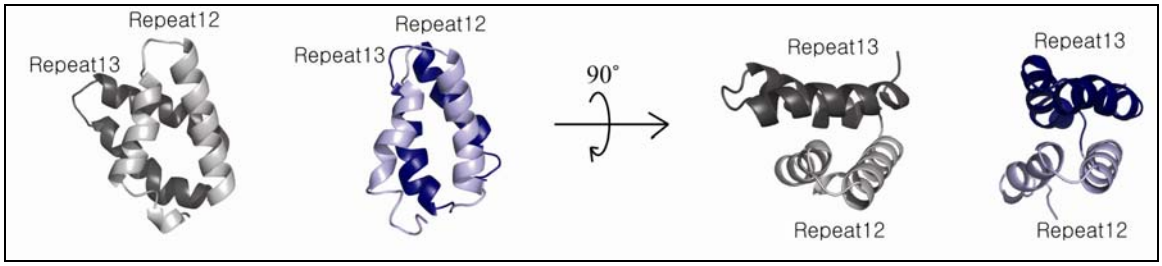


**Supplementary Figure S2. The structural detail in HEAT repeats 12 and 13 associated with the overall conformational change.** The Aα subunit alone is in gray and The Aα subunit in the trimeric complex is in blue. Repeat 12 is shown in lighter color than repeat 13.

## Supplementary Figure S3

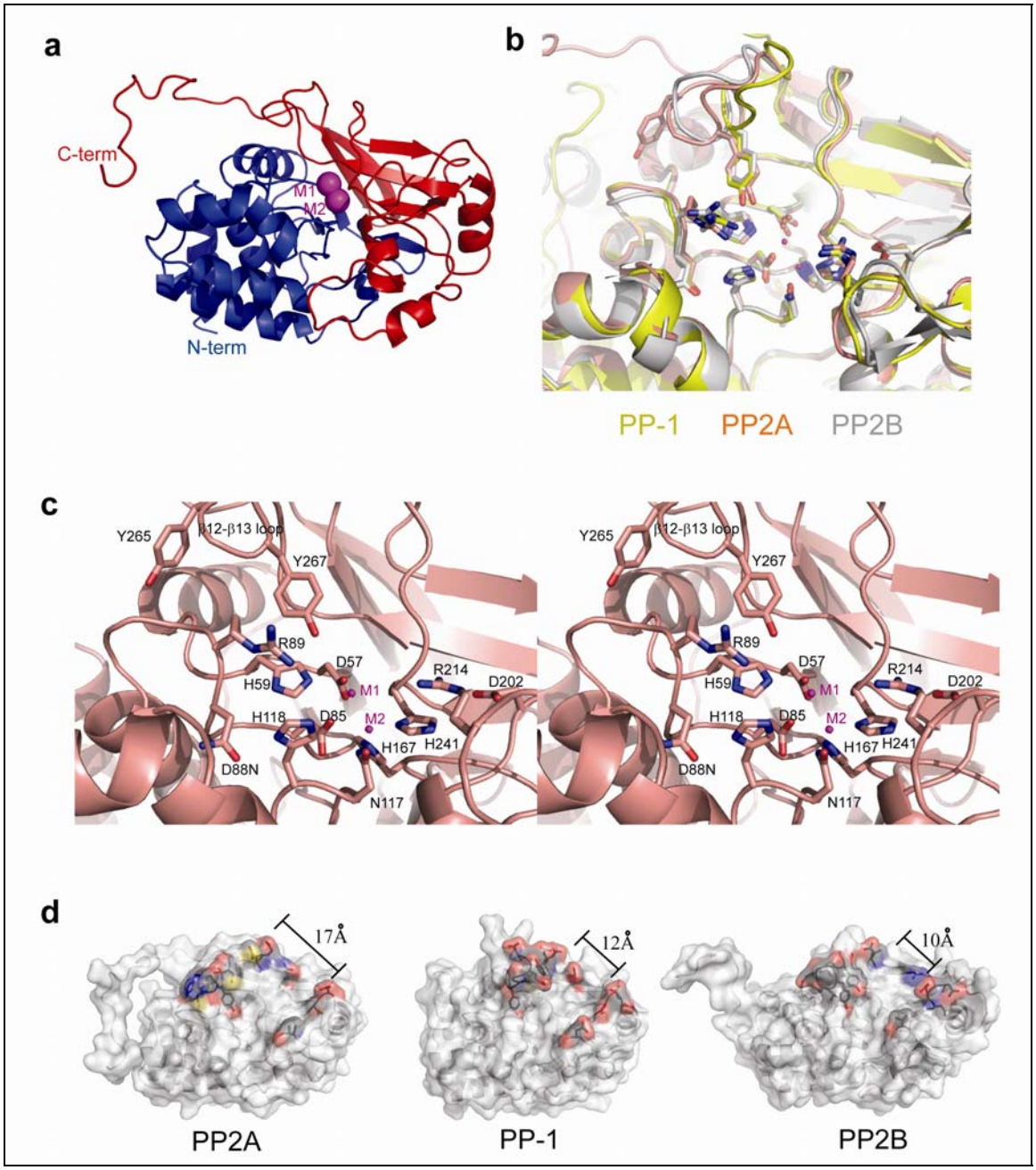


**Supplementary Figure S3. Structure of the catalytic Cα subunit. a,** The ribbon diagram of the Cα subunit. The N-terminal α/β and the C-terminal β-subdomains are in blue and red, respectively. Two metal ions are labeled M1 and M2 (purple). **b,** The superposition of active site residues among different Ser/Thr phosphatases. For better protein expression levels, we mutated residue Asp 88 in the PP2A active site to an Asn[42]. In the PP1 structure, the corresponding Asp 95 assists His 125 (His 118 in PP2A Cα subunit) by increasing its acidic character to donate $H^+$ to the Ser/Thr leaving group. The D88N mutation in PP2A is expected to decrease acidic character of H118 and prevent

proton donation. However, the overall positions of active site residues, including N88, are almost the same as those of PP1. **c,** A stereo-view of active-site residues in the catalytic Cα subunit. All active site residues of the PP2A Cα subunit except Tyr 265 are overlapped with those of PP1 and PP2B, including an active-site mutant D88N (see also the panel **b**). The position of conserved Tyr 265 is not in the catalytic active site. Instead, Tyr 267 sits at the same position with conserved Tyr residue in other phosphatases and may form part of the active site. The swap of these two Tyr positions may be induced by the interaction between R268 (β12-β13 loop) and long intra-repeat loop 2 of B56γ1. **d,** Comparison of the acidic groove in PP1, PP2A and PP2B. The electrostatic properties and the width of the acidic groove are varied on different phosphatases, which may provide different substrate specificity into each enzyme. The active site of PP1 is composed of the hydrophobic groove and the acidic groove, which are involved in inhibitor (e.g. microcystin) and substrate binding, respectively[44]. While the hydrophobic groove is highly conserved among PP2A, PP1 and PP2B, residues in the acidic groove are not conserved among different Ser/Thr phosphatases, which result in the different surface charge distribution and different width of the acidic groove. The width of the acidic groove in the PP2A C subunit (~17 Å) is wider than that of PP-1 (~12 Å) and PP2B (~10 Å). Acidic and basic residues are colored in red and blue, respectively. In addition to the acidic groove, the β12-β13 loop in PP2A C subunit has been shown to be important in the PP2A inhibitor recognition and may play a role in substrate recruitment.

## Supplementary Figure S4

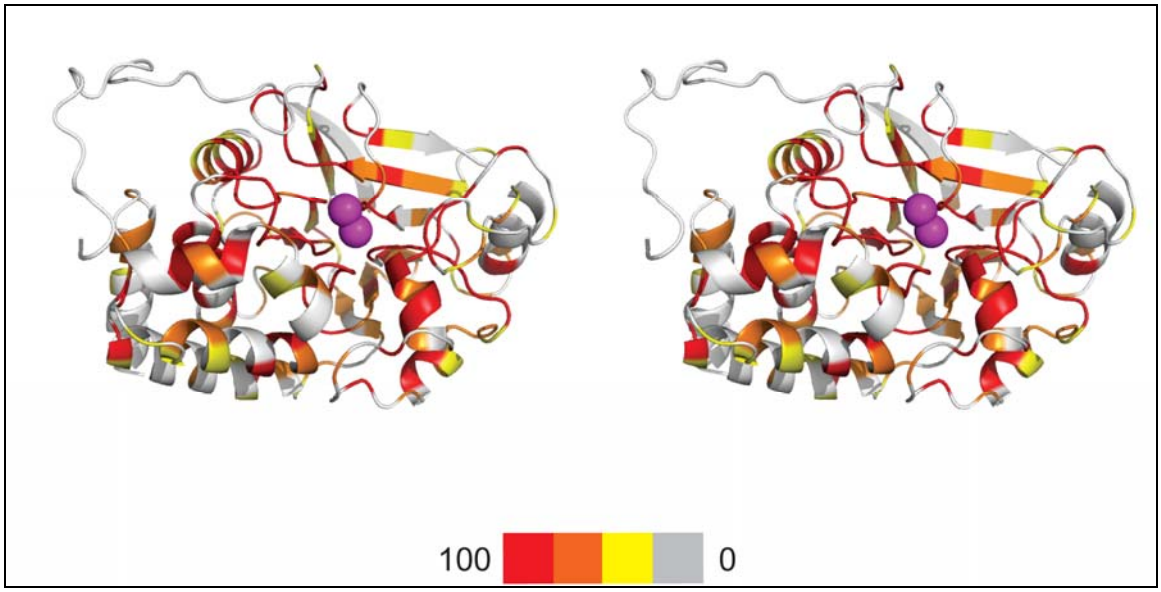


**Supplementary Figure S4. Stereo view showing spatial sequence conservation among PP2A, PP1 and PP2B.** The conservation level is demonstrated by color code. It is clear that most residues in the active site (e.g. involved in metal binding) and hydrophobic groove are highly conserved, while the sequence of the C-terminal tail is different.

## Supplementary Figure S5

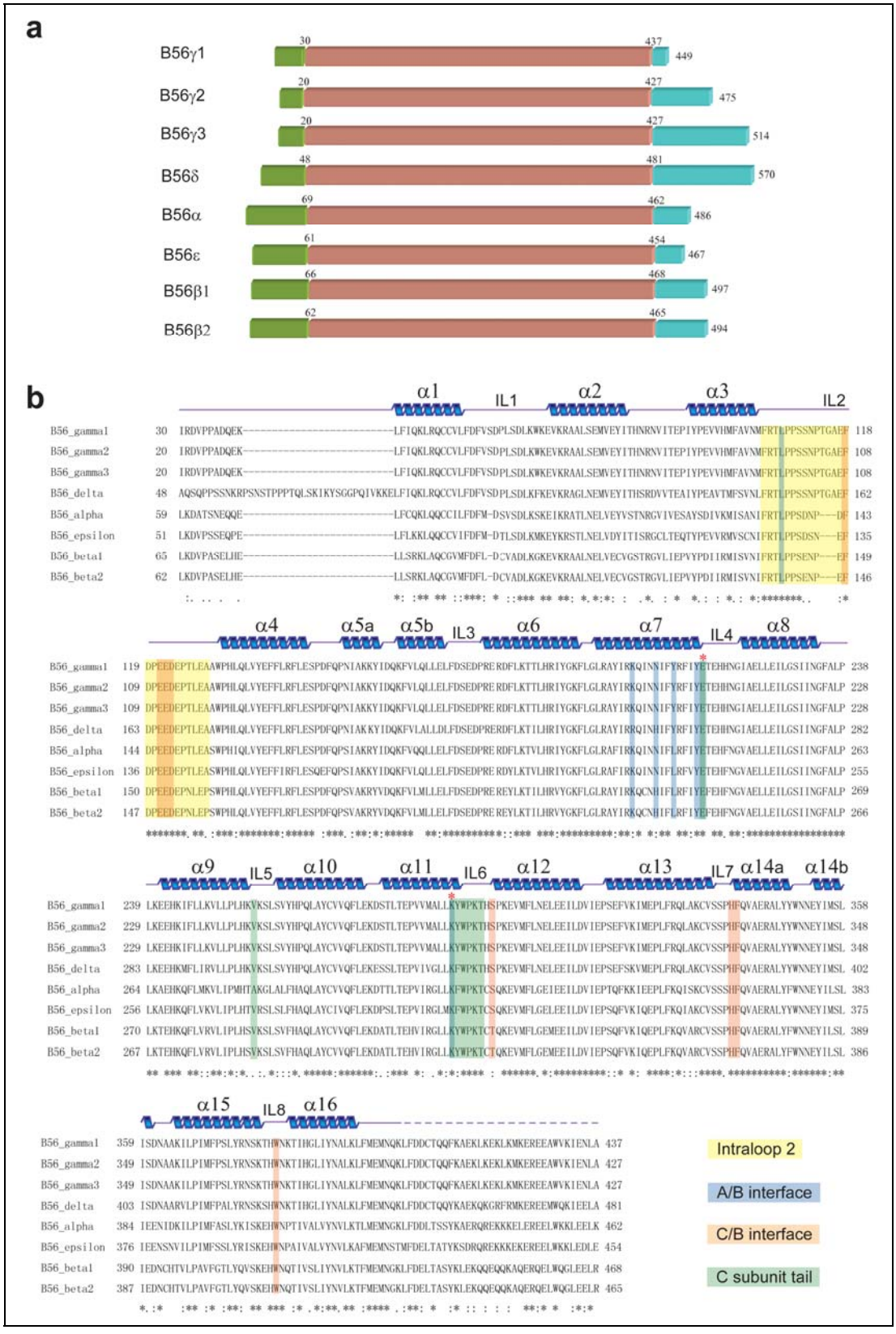

**Supplementary Figure S5. Sequence alignment of B'/B56 isoforms. a,** The schematic representation of the domain organization of B56 isoforms. The central conserved region of B56 isoforms is colored in orange, and divergent N-terminal and C-terminal regions are colored green and cyan, respectively. B56γ1(30-437) used in crystal structural determination lacks the N-terminal 29 residues and the C-terminal 12 residues. **b,** The sequence alignment of the central conserved region of B56 isoforms. Intra-repeat loop regions of each pseudo-HEAT repeat are labeled IL1 - IL8. The yellow box shows residues in the intra-repeat loop 2 region involved in the interaction with the β12-β13 loop of the catalytic Cα subunit. The blue box shows B56γ1 residues involved in the A-B interaction. The orange box represents B56γ1 residues involved in the B-C interaction. The green box represents contacting residues of B56γ1 involved in the C-terminal tail interaction. Red asterisks indicate two residues involved in both A-B and C-terminal tail interactions. The residues in the A-B interface appear less conserved than those in the B-C and C-terminal tail interface.

## Supplementary Figure S6

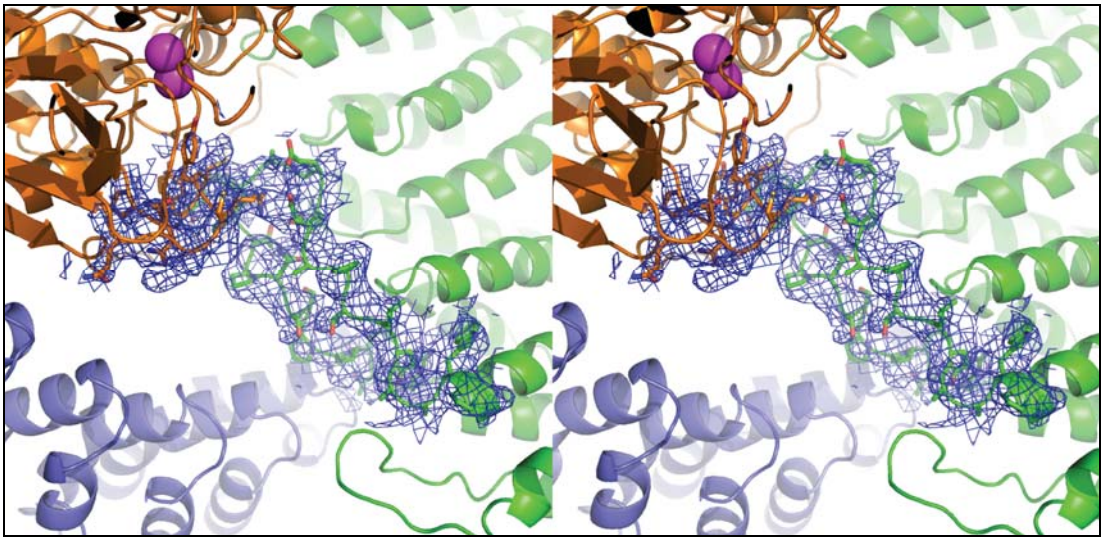

**Supplementary Figure S6. Electron density map of the intra-repeat loop 2 of B56γ1 and the β12-β13 loop of the C subunit.** A stereo-view of the initial experimental SAD electron density map contoured with 1σ level. The long intra-repeat loop 2 of B56γ1 is clearly shown in the density map.

## Supplementary figure S7

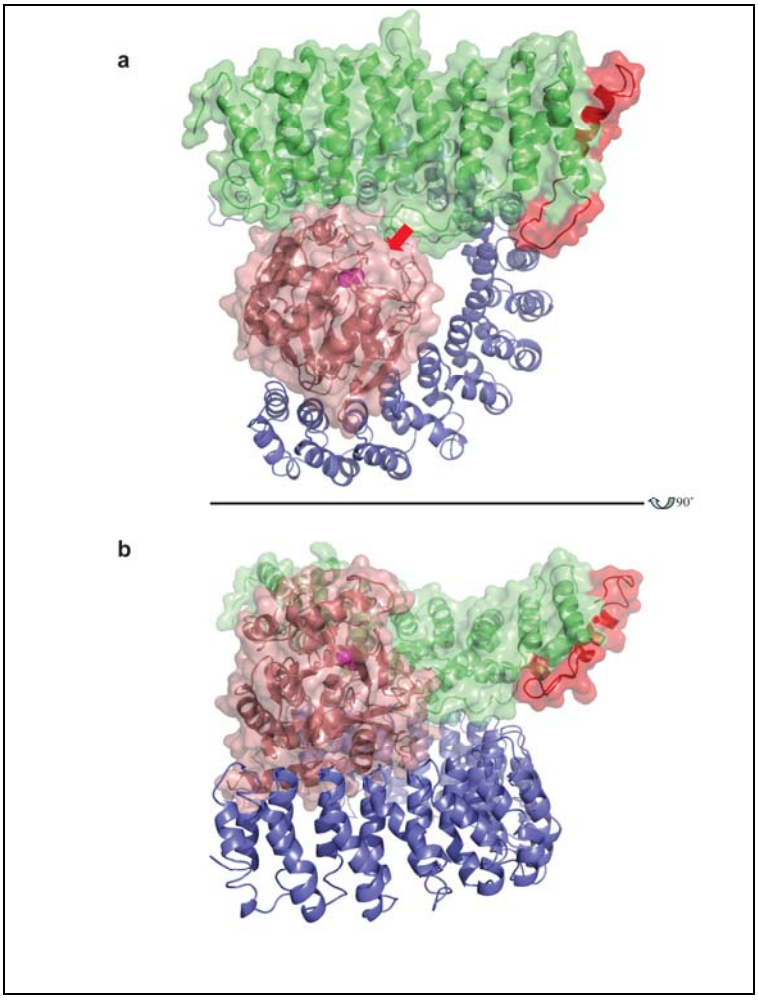


**Supplementary Figure S7. Structural basis of B56(Δγ1) mutation observed in cancer cells.** The B56(Δγ1) mutation, which lacks the N-terminal 65 residues of B56γ1 (shown in red), is found in the highly metastatic BL6 mouse melanoma cell line. This B56 mutant retains the ability to interact with the PP2A AC core, but changes its activity towards some important targets in the cell, including paxillin and mdm2[45, 46]. Consistent with these functional studies, the first 65 B56γ1 residues are not involved in direct interaction with the A and C subunits in our crystal structure. These residues of B56γ1 may instead be involved in paxillin or mdm2 binding. Alternatively, this deletion might affect substrate recognition by changing the conformation of the B56γ1 intra-repeat loop 2, since it interacts with the long intra-repeat loop 1 included in the first 65 residues. It is interesting to note that the long intra-repeat loop 2 of B56γ1 interacts with the C subunit β12-β13 loop that is particularly important to inhibitor recognition in PP2A and PP1[47-50]. It is possible that the connection between intra-repeat loop 2 and the C subunit β12-β13 loop also plays a role in substrate specificity. The intra-repeat loop 2 is the most variable region in the B56 core domain (Supplementary Fig. S5b), and may be important for substrate selectivity among different B56 members.

## Supplementary figure S8

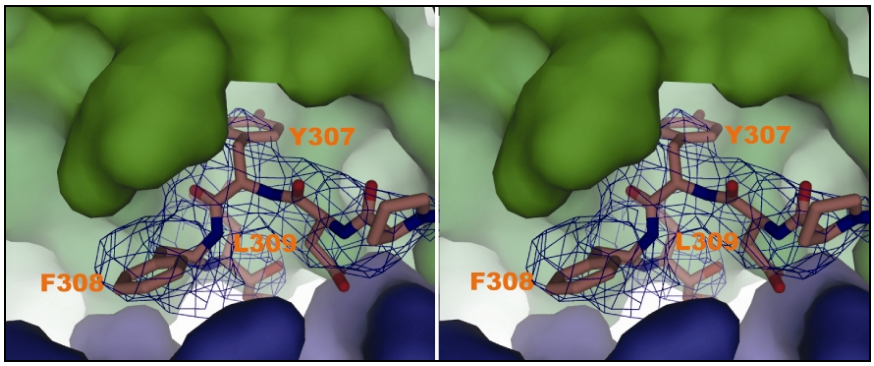


**Supplementary Figure S8. Structural basis of PP2A regulation by the phosphorylation of C subunit Tyr307.** PP2A activity can be also inhibited by the phosphorylation of Tyr 307 via tyrosine kinases such as Src[51]. In our structure, the side chain of Tyr 307 of the C-terminal tail interacts with a pocket formed by the B56γ1 subunit and forms a hydrogen bond with the main chain carbonyl of Val 257 of the B subunit (see also Fig. 5a). The phosphorylation of Tyr 307 would likely disrupt the interaction between the C-terminal tail and the B subunit and thus prevent PP2A assembly. Alternatively, the C-terminal tail with phosphorylated Tyr 307 may inhibit PP2A activity through direct interaction with the C subunit active site, a favorite model proposed for PP5 regulation[52]. Future work is needed to examine these two non-exclusive models. In this figure, the structural surface of the A and B subunits and the initial SAD experimental electron density map for the C-terminal tail contoured at 1σ level. The methylated C-terminal tail of the Cα subunit is shown in sticks.

## Supplementary figure S9

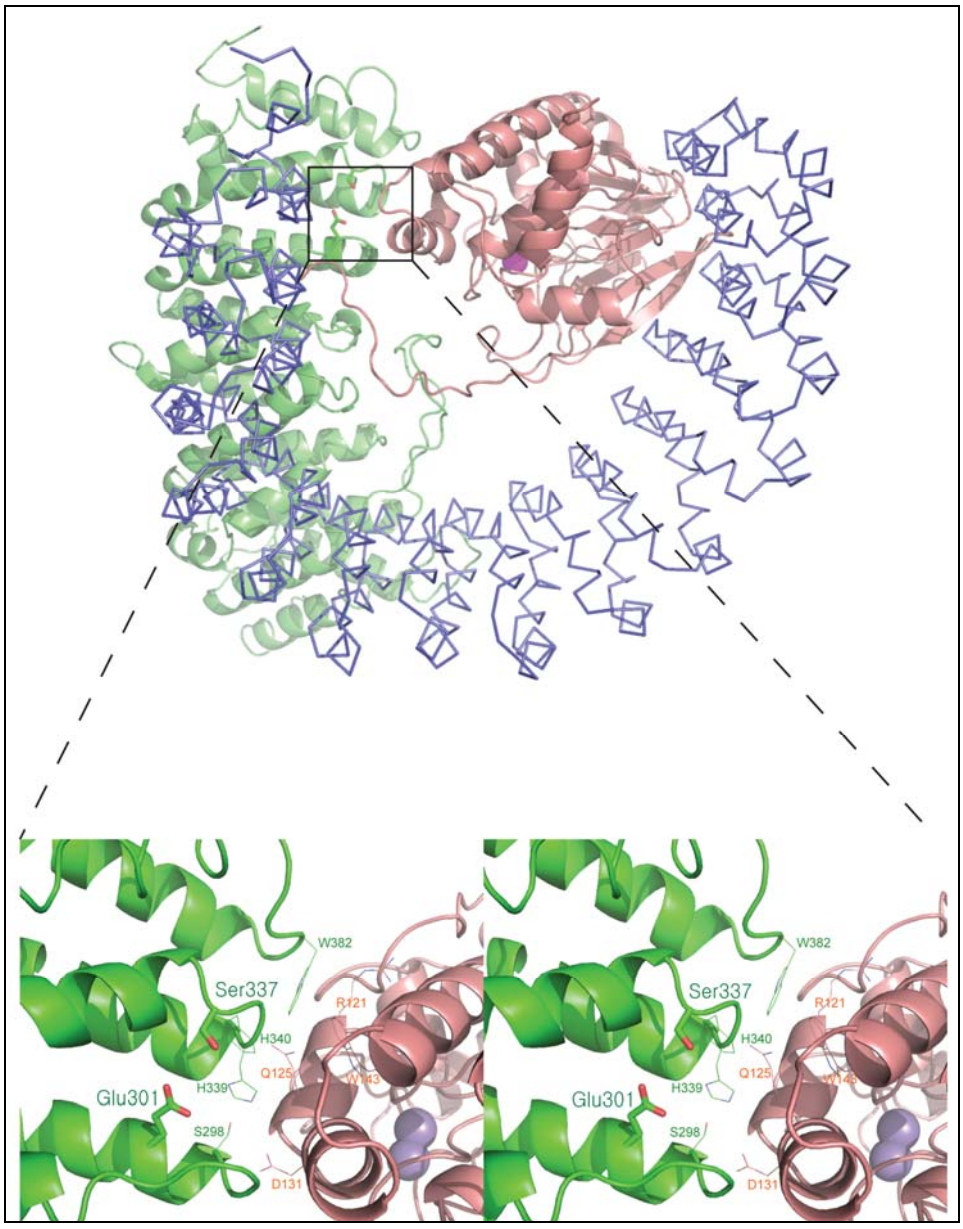


**Supplementary Figure S9. Structural basis of Erk-regulated PP2A assembly.** It has been shown that the MAP kinase ERK inhibits PP2A AB'C activity by phosphorylating a conserved Ser residue (Ser 337 in B56γ1) in a B subunit HEAT repeat that disrupts the interaction between B56 and the AC core enzyme[53]. In our crystal structure, Ser 337 is located in the intra-repeat loop 7, the center of the B-C interface (also see Fig. 4a). Phosphorylation of Ser337 is likely to induce a conformational change in this area since the phosphate group of Ser 337 would be otherwise colliding with the acidic residue Glu 301. Any conformational change in the intra-repeat loop 7 would directly affect B-C interaction.

## References


41. Wadzinski, B. E., Eisfelder, B. J., Peruski, L. F., Jr., Mumby, M. C. & Johnson, G. L. NH2-terminal modification of the phosphatase 2A catalytic subunit allows functional expression in mammalian cells. *J. Biol. Chem.* **267**, 16883-16888 (1992).
42. Myles, T., Schmidt, K., Evans, D. R., Cron, P. & Hemmings, B. A. Active-site mutations impairing the catalytic function of the catalytic subunit of human protein phosphatase 2A permit baculovirus-mediated overexpression in insect cells. *Biochem. J.* **357**, 225-232 (2001).
43. Ikehara, T., Shinjo, F., Ikehara, S., Imamura, S. & Yasumoto, T. Baculovirus expression, purification, and characterization of human protein phosphatase 2A catalytic subunits alpha and beta. *Protein Expr. Purif.* **45**, 150-156 (2006).
44. Goldberg, J. et al. Three-dimensional structure of the catalytic subunit of protein serine/threonine phosphatase-1. *Nature* **376**, 745-753 (1995).
45. Ito, A. et al. A truncated isoform of the PP2A B56 subunit promotes cell motility through paxillin phosphorylation. *EMBO J.* **19**, 562-571 (2000).
46. Koma, Y. I., Ito, A., Watabe, K., Kimura, S. H. & Kitamura, Y. A truncated isoform of the PP2A B56gamma regulatory subunit reduces irradiation-induced Mdm2 phosphorylation and could contribute to metastatic melanoma cell radioresistance. *Histol. Histopathol.* **19**, 391-400 (2004).
47. Shima, H. et al. Characterization of the PP2A alpha gene mutation in okadaic acid-resistant variants of CHO-K1 cells. *Proc. Natl. Acad. Sci. USA* **91**, 9267-9271 (1994).
48. Kaneko, S. et al. Analysis by in vitro mutagenesis of PP2A alpha okadaic acid responsive sequences. *Biochem. Biophys. Res. Commun.* **214**, 518-523 (1995).
49. Connor, J. H., Kleeman, T., Barik, S., Honkanen, R. E. & Shenolikar, S. Importance of the beta12-beta13 loop in protein phosphatase-1 catalytic subunit for inhibition by toxins and mammalian protein inhibitors. *J. Biol. Chem.* **274**, 22366-22372 (1999).
50. Kita, A. et al. Crystal structure of the complex between calyculin A and the catalytic subunit of protein phosphatase 1. *Structure* **10**, 715-724 (2002).
51. Chen, J., Martin, B. L. & Brautigan, D. L. Regulation of protein serine-threonine phosphatase type-2A by tyrosine phosphorylation. *Science* **257**, 1261-1264 (1992).
52. Yang, J. et al. Molecular basis for TPR domain-mediated regulation of protein phosphatase 5. *EMBO J.* **24**, 1-10 (2005).
53. Letourneux, C., Rocher, G. & Porteu, F. B56-containing PP2A dephosphorylate ERK and their activity is controlled by the early gene IEX-1 and ERK. *EMBO J.* **25**, 727-738 (2006).